基于UPLC-QTOF-MS/MS和网络药理学分析大补肺汤体−用−化配伍治疗COPD稳定期的物质基础和作用机制

韩　昱[1], 罗月月[1], 黄圣如[1], 宿树兰[1*], 刘　培[1], 尚尔鑫[1], 刘永琦[2], 段金廒[1]

(1. 南京中医药大学, 江苏省方剂功效物质与创新药物发现重点实验室, 中药资源产业化与方剂创新药物国家地方联合工程研究中心, 江苏省中药资源产业化过程协同创新中心, 中药制药过程控制与智能制造技术全国重点实验室, 江苏 南京 210023;　2. 甘肃中医药大学, 敦煌医学与转化教育部重点实验室, 甘肃 兰州 730050)

摘要: 采用超高效液相−四级杆−飞行时间高分辨质谱联用 (UPLC-QTOF-MS/MS) 技术对大补肺汤的化学成分进行分析和鉴定, 并结合网络药理学探究大补肺汤作用于慢性阻塞性肺疾病 (chronic obstructive pulmonary disease, COPD) 稳定期的作用机制。在正、负离子模式下, 通过化合物精确分子量、MS/MS裂解规律和文献报道数据等信息对大补肺汤中的化学成分进行鉴定, 再结合TCMSP数据库、文献挖掘大补肺汤有效成分和作用靶点, 通过OMIM、Gene Cards数据库获得COPD稳定期靶点, 筛选出药物靶点和疾病靶点的交集靶点, 导入STRING数据库及Cytoscape 3.10.3构建PPI网络, 通过Metascape数据库对核心靶点进行GO和KEGG富集分析。结果显示, 大补肺汤中共鉴定出132个化学成分, 有87种成分来自“用”组药味, 49种来自“体”组药味, 4种来自“化”组药味, 8种成分为体、用组药味共有成分。基于Swiss ADME胃肠道吸收和类药性五项原则筛选出大补肺汤中84个潜在活性成分, 与COPD稳定期有294个共同靶点, 基于Cytoscape计算得到87个核心靶点, KEGG富集通路主要包括PI3K-AKT信号通路、HIF-1α信号通路、AGE-RAGE信号通路、EGFR酪氨酸激酶抑制剂耐药性、MAPK信号通路等发挥治疗COPD稳定期的作用, 其中体组药味主要作用于C型凝集素受体信号通路, 用组药味作用于PI3K-AKT信号通路, 化组药味作用于Th17细胞的分化过程。研究结果为该方临床应用及深入研究提供科学依据与支撑。

关键词: 大补肺汤; 慢性阻塞性肺疾病稳定期; 网络药理; 化学成分; 作用机制; 辅行诀

中图分类号: R917　　**文献标识码**: A　　**文章编号**: 0513-4870(2026)05-1804-15

Study on the material basis and mechanism of "Ti-Yong-Hua" compatibility of Dabufei Decoction in treating the stable phase of COPD based on UPLC-QTOF-MS/MS and network pharmacology

HAN Yu[1], LUO Yue-yue[1], HUANG Sheng-ru[1], SU Shu-lan[1*], LIU Pei[1], SHANG Er-xin[1], LIU Yong-qi[2], DUAN Jin-ao[1]

(*1. Nanjing University of Chinese Medicine, Jiangsu Key Laboratory for High Technology Research of Traditional Chinese Medicine Formulae, National-Local Joint Engineering Research Center of Resources Industrialization of Chinese Medica and Prescription-Oriented Innovative Drugs, Jiangsu Collaborative Innovation Center of Chinese Medicinal Resources Industrialization, State Key Laboratory of Technologies for Chinese Medicine Pharmaceutical Process Control and Intelligent Manufacture, Nanjing 210023, China;　2. Gansu University of Chinese Medicine, Dunhuang Key Laboratory of Medicine and Traditional Education of the Ministry of Education, Lanzhou 730050, China*)

Abstract: Ultra-high performance liquid chromatography-quadrupole-time-of-flight tandem mass spectrometry

收稿日期: 2025-10-30;　修回日期: 2026-01-11.

基金项目: 国家自然科学基金区域创新发展联合基金重点支持项目 (U23A20502); 国家中医药管理局高水平中医药重点学科建设项目 (ZYYZDXK-2023083); 江苏省高校优秀科技创新团队项目 (2021); 敦煌医学与转化教育部重点实验室开放课题 (DHYX23-01).

*通讯作者 E-mail: sushulan@njucm.edu.cn

DOI: 10.16438/j.0513-4870.2025-1278

(UPLC-QTOF-MS/MS) was used to analyze and identify the chemical components of Dabufei Decoction (DBFT). Combined with network pharmacology, the mechanism of action of DBFT in the stable phase of chronic obstructive pulmonary disease (COPD) was explored. Under positive and negative ion modes, the chemical components of DBFT were identified based on information such as the accurate molecular weight of compounds, MS/MS fragmentation rules, and literature-reported data. Then, combined with the TCMSP database and literature mining, the active components and action targets of DBFT were obtained. Targets related to the stable phase of COPD were retrieved from the OMIM and Gene Cards databases. The overlapping targets between drug targets and disease targets were screened out, imported into the STRING database and Cytoscape 3.10.3 to construct a protein-protein interaction (PPI) network, and Gene Ontology (GO) and Kyoto Encyclopedia of Genes and Genomes (KEGG) enrichment analyses of core targets were performed using the Metascape database. The results showed that a total of 132 chemical components were identified in DBFT, among which 87 components were derived from the "Yong" group of herbs, 49 from the "Ti" group of herbs, 4 from the "Hua" group of herbs, and 8 components were shared by the "Ti" and "Yong" groups of herbs. A total of 84 potential active components of DBFT were screened out based on the Swiss ADME gastrointestinal absorption and five principles of druggability. There were 294 common targets with the stable phase of COPD, and 87 core targets were obtained through calculation using Cytoscape. The KEGG-enriched pathways mainly included the PI3K-AKT signaling pathway, HIF-1α signaling pathway, AGE-RAGE signaling pathway, EGFR tyrosine kinase inhibitor resistance, and MAPK signaling pathway, which played a role in the treatment of the stable phase of COPD. Among them, the "Ti" group of herbs mainly acted on the C-type lectin receptor signaling pathway, the "Yong" group of herbs acted on the PI3K-AKT signaling pathway, and the "Hua" group of herbs acted on the differentiation process of Th17 cells. The research results provide a scientific basis and support for the clinical application and in-depth study of this prescription.

Key words: Dabufei Decoction; stable phase of chronic obstructive pulmonary disease; network pharmacology; chemical component; mechanism of action; Fuxingjue

慢性阻塞性肺疾病 (chronic obstructive pulmonary disease, COPD), 简称慢阻肺, 是一种异质性疾病, 特征主要为慢性呼吸道症状 (呼吸困难、咳嗽、咳痰), 这是由于气道 (支气管炎、细支气管炎) 和/或肺泡异常 (肺气肿) 所致, 引起持续加重的气流受限[1]。全球疾病负担 (global burden of disease, GBD) 的数据显示, COPD全球患病率为10.3%[2-4], 我国40岁及以上成年人患病率高达13.7%, 且随着人口老龄化的加剧和吸烟率的上升, 慢阻肺的患病率在未来呈现持续上升的趋势[5]。目前, 我国慢阻肺的治疗多采用吸入支气管舒张剂、口服β_2受体激动剂、茶碱类药物等方法, 但不良反应明显, 易引起心动过速、心律失常、肌肉震颤等问题。近年来, 研究表明中医药能够通过调控炎症反应、改善免疫调节、降低氧化应激等多途径治疗COPD。

《辅行诀脏腑用药法要》是一部总结商代伊尹的《汤液经法》辨五脏病证及组方用药规律的书籍, 以“汤液经法图”作为组方配伍的核心机制, 基于五脏虚实辨证采用五味体用补泻的治疗方法[6,7]。《辅行诀》认为病因正气亏损而成, 治法着力于调和五脏体用之平衡, 其中蕴含着富有特色的“体–用–化”治法理论。《辅行诀》中提及的脏之体和用, 根据《素问·脏气法时论》中天人合一的思想, 可认为用为五脏的功用, 体为发生功用的物质基础, 简而言之, 脏之用是不可见的、偏功能性的现象, 脏之体是可见的、有形质的物质基础[8]。脏之化为调和, 虚实兼治, 为五味配伍转换关系, 即在体用交换过程中, 体用合二为一而形成的新的质体, 以平和脏腑。COPD稳定期在中医论治中属于“肺虚”, 从《辅行诀》补泻治法来看, 虚需补之, 补本脏或补母脏, 故重用用味、轻用体味。大补肺汤由五味子、麦冬、生地黄、淡竹叶、旋覆花、炙甘草、细辛7味药组成, 共四补两泻一化, 主治烦热汗出, 少气不足息, 口干、耳聋, 脉虚而快。其中, 五味子补肺用; 麦冬补母脏脾土; 地黄、竹叶, 补子脏肾水; 旋覆花泻肺体, 以防滋腻; 甘草补母脏, 培土生金; 细辛入肺脏化味, 调肺虚[9,10]。目前, 对于大补肺汤治疗慢阻肺稳定期的药效物质基础及其作用机制研究尚不深入。

根据课题组[11]前期研究, 本文基于UPLC-Q-TOF-MS/MS技术对大补肺汤的化学成分进行分析鉴定, 通过网络药理学方法对大补肺汤及体、用、化各组治疗慢阻肺稳定期的潜在活性成分及分子机制进行预测分析, 以期为大补肺汤的临床应用和深入研究提供科学依据。

材料与方法

仪器　UPLC-Q-TOF-MS/MS (ESI) 串联质谱仪、MassLynx™ v4.2 (Waters Corp.) 分析软件、Waters

ACQUITY UPLC系统 (包括四元泵溶剂, 在线脱气机和自动进样器; 美国Waters公司); AB Triple Quad 6500 Plus三重四级杆线性离子阱质谱仪系统 (美国AB SCIEX公司), 配有电喷雾离子源及Analyst1.6.3软件; 微型涡旋混合仪 (上海沪西分析仪器厂有限公司); ML105型电子天平 (赛多利斯科学仪器北京有限公司); Unique-R40多功能超纯水系统 (厦门锐思捷水纯化技术有限公司); Anke GL-16G型离心机 (上海安亭科学仪器厂)。

药品与试剂 大补肺汤中五味子 (批号240401, 产地辽宁)、麦冬 (批号240316, 产地四川)、生地黄 (批号240320, 产地河南)、淡竹叶 (批号240119, 产地浙江)、旋覆花 (批号240115, 产地江苏)、炙甘草 (批号240315, 产地内蒙古)、细辛 (批号240228, 产地辽宁) 7味药材均购自苏州市天灵中药饮片有限公司, 经南京中医药大学段金廒教授鉴定为正品药材饮片。对照品五味子甲素 (批号: J10GB151096)、五味子丙素 (批号: N04GB166743)、五味子醇乙 (批号: JB247585)、甲基麦冬黄酮A (批号: A28IB214114)、麦冬黄烷酮A (批号: F26HB176323)、1-*O*-乙酰旋覆花内酯 (批号: KB356710)、大花旋覆花素 (批号: Z04A9L57509)、克拉霉素(批号: Y31M7C12157)均购自上海源叶生物科技有限公司。色谱级乙腈和甲醇 (德国Merck公司), 色谱级甲酸 (美国Thermo Fisher Scientific公司), 屈臣氏蒸馏水购自南京何苗生物科技有限公司。

对照品溶液 称取适量对照品五味子醇乙、五味子甲素、五味子丙素、甲基麦冬黄酮A、麦冬黄烷酮A、1-*O*-乙酰旋覆花内酯、大花旋覆花素加甲醇溶解后定容, 混匀, 即得单一成分对照品储备液。

标准曲线溶液 精密吸取对照品溶液储备液适量, 混匀制成混合标准品溶液, 并用甲醇稀释成一系列浓度, 得到定量标准曲线溶液。

标准曲线溶液 精密称取对照品克拉霉素适量, 用甲醇溶解并稀释至500 ng·mL^{-1}作为内标溶液。

供试品溶液 根据该方的临床用法, 采用水煎煮的方法进行样品制备。称取五味子9 g、麦冬9 g、生地黄3 g、淡竹叶3 g、旋覆花9 g、炙甘草3 g、细辛3 g, 第一次加入10倍量水浸泡30 min, 沸腾后煎煮1 h, 过滤收集药液, 再加入10倍量水煎煮1 h, 过滤合并滤液, 浓缩至每1 mL含1 g生药的大补肺汤水提液样品。精密吸取大补肺汤水提液样品1 mL, 加入4 mL甲醇后涡旋混匀, 4 ℃下13 000 r·min^{-1}离心15 min, 取上清液经0.22 μm孔径滤膜过滤得供试品溶液, 备用。

色谱条件 采用Waters ACQUITY UPLC BEH C_{18}色谱柱 (100 mm × 2.1 mm, 1.7 μm); 流动相: 0.1%甲酸水 (A)−乙腈 (B); 梯度洗脱: 0～3 min, 5%～30% B; 20～22 min, 30%～100% B; 22～24 min, 100%～5% B; 24～25 min, 5% B; 柱温: 30 ℃; 流速: 0.4 mL·min^{-1}; 进样量: 2 μL。

UPLC-Q-TOF-MS/MS质谱条件 采用电喷雾离子源 (ESI) 正、负离子扫描模式, 毛细管电压3.0 kV, 离子源温度120 ℃, 脱溶剂温度400 ℃, 锥孔电压15 V, 锥孔气流量50 L·h^{-1}, 脱溶剂流量80 L·h^{-1}, 质量扫描范围 *m*/*z* 100～1 000, MS/MS源内碰撞诱导解离电压为20～30 V。

AB Triple Quad 6500 Plus质谱条件 采用电喷雾离子源 (ESI) 正离子扫描模式, 检测模式为多反应检测 (MRM) 模式, 正离子电喷雾电压: 5 500 V, 雾化气压力40 kPa, 气帘气压力40 kPa, 离子源温度450 ℃, 碰撞气: Medium, 7种被测物质及1种内标物质MRM参数见表1。

Table 1 Mass spectrum parameters of each component. DP: Declustering potential; CE: Collision energy

Component	Polarity	*m*/*z*		DP/V	CE/V
		Precursor ion	Product ion		
Schisandrol B	ES^+	416.1	314.2	66	37
Schizandrin A	ES^+	417.2	316.2	6	35
Schisandrin C	ES^+	385.1	285.2	206	33
Methylophiopogonone A	ES^+	341.1	219.3	1	31
Ophiogonanone A	ES^+	330.1	136.3	11	25
1-*O*-Acetyl britannilactone	ES^+	309.2	185.4	11	23
Britannin	ES^+	367.1	247.3	56	15
Clarithromycin	ES^+	748.5	590.3	41	29

线性关系考察 对不同浓度混合对照品溶液进样测定, 以对照品与内标峰面积之比为纵坐标 (*Y*), 以各成分质量浓度 (ng·mL^{-1}) 为横坐标 (*X*) 进行线性回归, 绘制标准曲线, 结果见表2, 可知各成分在各自浓度范围内线性关系良好。

大补肺汤活性成分的获取 选取UPLC-Q-TOF-MS/MS鉴定的全部成分为目标成分, 并结合TCMSP、中国知网 (https://www. cnki. net)、PubMed (https://pubmed.ncbi.nlm.nih.gov) 等数据库, 筛选条件为类药性 (drug-likeness, DL) ≥ 0.18, 口服生物利用度 (oral bioavailability, OB) ≥ 30%, 在Pub Chem数据库 (https://pubchem.ncbi.nlm.nih.gov/) 中检索各成分的SDF结构与SMILES号, 在Swiss ADME (http://www.swissadme.ch/) 中以GI absorption=High, Lipinski、Ghose、Veber、Egan、Muegge中两种及以上类药性原则为“yes”为条件进一步筛选获得潜在活性成分。

疾病靶点预测 分别在Gene Cards数据库 (https://www. genecards. org/)、OMIM数据库 (https://www.omim.org/) 中, 以慢性阻塞性肺疾病稳定期 (stable

Table 2　Mass spectrum parameters of each component

Component	Linear regression equation	r^2	Linear range/ng·mL^{-1}
Schisandrol B	Y = 1 117.3X − 2 346.5	0.992 1	12.207−195.312
Schizandrin A	Y = 280 477X − 554 583	0.999 6	6.470−103.516
Schisandrin C	Y = 1 157.9X − 10 010	0.999 3	6.104−781.250
Methylophiopogonone A	Y = 264 984X − 1 000 000	0.999 8	5.920−378.906
Ophiogonanone A	Y = 1 076.6X − 7 745.3	0.998 2	11.963−382.812
1-*O*-Acetyl britannilactone	Y = 13 159X − 119 404	0.999 5	6.287−804.687
Britannin	Y = 2 888.7X − 8 384.8	0.997 3	6.714−214.844

phase of chronic obstructive pulmonary disease) 为关键词进行搜索, 取Gene Cards数据库前25%的靶点, 整合所有靶点并去重, 得到COPD稳定期的靶点。

疾病蛋白相互作用网络及“成分−靶点”网络的构建　利用Jvenn网站分别对拆方各组作用靶点与COPD稳定期取交集, 将交集靶点分别导入STRING数据库(https://cn.string-db.org/), Organisms选择“homo sapiens”, “minimum required interaction score”选择0.9, 构建蛋白相互作用 (protein-protein interaction, PPI) 网络, 将数据导入Cytoscape 3.10.3软件进行分析, 根据度值(degree)、中介中心性 (betweenness centrality, BC)、接近中心性 (closeness centrality, CC) 筛选出大补肺汤改善COPD稳定期的核心靶点。运用Cytoscape 3.10.3软件构建“成分−靶点”网络图, 并筛选得到大补肺汤及其各组分发挥药效的核心成分。

作用靶点基因富集分析　对上述取得的作用靶点基因进行富集分析, 将筛选出的靶点导入Metascape数据库 (https://metascape.org/gp/index.html/) 进行GO生物功能富集分析和KEGG通路富集分析, 以P < 0.05为显著性结果。

结果

1　大补肺汤化学组成分析

1.1　大补肺汤化学成分定性分析

采用UPLC-Q-TOF-MS/MS技术对大补肺汤中的化学成分进行定性分析, 总离子流图见图1。通过一级和二级质谱信息分析并结合相关文献及Pubchem数据库[12-18], 从大补肺汤样品图谱中共鉴定和表征出132个化学成分, 主要为苯丙素类、有机酸类、黄酮类、皂苷类、环烯醚萜类、酚酸类等成分, 见表3。其中, 有87种成分来自“用”组, 49种来自“体”组, 4种来自“化”组, 8种成分为体、用组共有成分。以上分析可以得知, 配伍后的化学成分呈现以体用为主的作用特点。

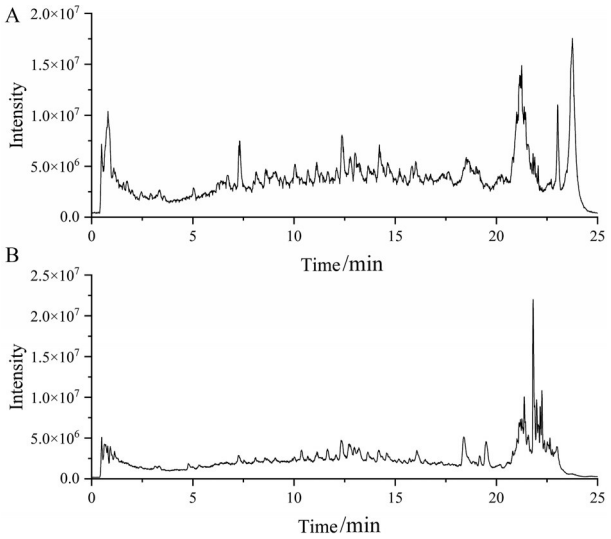


Figure 1　Total ion flow diagram of UPLC-QTOF-MS analysis. A: Negative ion mode; B: Positive ion mode

1.2　大补肺汤化学成分的质谱裂解特征分析

1.2.1　木脂素类化合物的鉴定　化合物128在正离子模式下检出, 保留时间为22.753 min, 准分子离子峰为m/z 417.226 5 $[M+H]^+$, 推测化学式为$C_{24}H_{32}O_6$。裂解时脱去CH_3生成m/z 402.203 2 $[M+H-CH_3]^+$, 后又再脱去O生成m/z 386.204 3 $[M+H-CH_3-O]^+$, 继续脱去CH_3生成m/z 371.184 9 $[M+H-CH_3-O-CH_3]^+$, 结合数据库

Table 3　Identification and analysis of the chemical constituents of Dabufei Decoction (DBFT). WWZ: Wuweizi; MD: Maidong; DZY: Danzhuye; SDH: Shengdihuang; XFH: Xuanfuhua; ZGC: Zhigancao; XX: Xixin

No.	Identification	t_R/min	Formula	Adducts	Precursor ion/m/z	Error /×10^6	Fragment ion/m/z	Origin plant
1	Verbascoside	0.589	$C_{30}H_{52}O_{26}$	$[M+Na]^+$	851.261 4	−3.6	689.212 4, 365.103 0, 163.064 4	Yong (SDH)
2	Rehmannioside A	0.888	$C_{21}H_{32}O_{15}$	$[M+Na]^+$	547.164 1	0.4	365.106 9, 238.074 4, 146.059 1	Yong (SDH)
3	Raffinose	0.930	$C_{18}H_{32}O_{16}$	$[M+Na]^+$	527.159 3	0.9	325.116 5, 163.063 5	Yong (SDH)
4	Adenine	0.940	$C_5H_5N_5$	$[M+H]^+$	136.062 1	−1.5	119.035 4	Yong (MD)
5	2′-Acetylacteoside	0.982	$C_{31}H_{38}O_{16}$	$[M+Na]^+$	689.204 2	−2.3	649.194 1, 365.111 4, 325.110 3	Yong (SDH)
6	Fructose	0.992	$C_6H_{12}O_6$	$[M+Na]^+$	203.052 5	−3.4	163.058 3, 145.048 8, 127.039 5	Yong (SDH)

Continued

No.	Identification	t_R /min	Formula	Adducts	Precursor ion/*m*/*z*	Error /×10^6	Fragment ion/*m*/*z*	Origin plant
7	Adenosine	1.063	$C_{10}H_{13}N_5O_4$	$[M+H]^+$	268.105 3	2.6	136.060 6, 119.033 8	Yong (SDH)
8	Arginine	3.729	$C_6H_{14}N_4O_2$	$[M+H]^+$	175.120 0	2.9	112.084 3, 116.069 9	Hua (XX)
9	Citric acid	1.457	$C_6H_8O_7$	$[M-H]^-$	191.020 1	4.7	111.009 6	Yong (WWZ, SDH)
10	Stachyose	1.528	$C_{24}H_{42}O_{21}$	$[M+H]^+$	667.228 7	−1.5	527.156 9, 275.078 6, 203.057 1	Yong (SDH)
11	Catalpol	1.538	$C_{15}H_{22}O_{10}$	$[M+Na]^+$	385.112 3	3.1	136.061 5, 119.034 6	Yong (SDH)
12	Rehmannioside D	1.693	$C_{27}H_{42}O_{20}$	$[M-H]^-$	685.219 8	1.0	505.149 9, 341.112 9, 263.077 6, 179.055 3	Yong (SDH)
13	Melittoside	1.995	$C_{21}H_{32}O_{15}$	$[M-H]^-$	523.167 5	2.3	163.041 3, 135.045 9	Yong (SDH)
14	Protocatechuic acid	2.139	$C_7H_6O_4$	$[M-H]^-$	153.019 4	3.9	109.028 8	Ti (XFH), Yong (WWZ, DZY, SDH)
15	Geniposidic acid	2.139	$C_{16}H_{22}O_{10}$	$[M-H]^-$	373.112 6	−2.4	211.061 2, 123.048 7	Yong (SDH)
16	Dihydroferulic acid	2.758	$C_{10}H_{12}O_4$	$[M+H]^+$	197.081 5	0.5	179.072 9, 167.071 4	Yong (SDH)
17	Salidroside	2.779	$C_{14}H_{20}O_7$	$[M+Na]^+$	323.109 6	−3.4	224.061 5	Yong (SDH)
18	Vanillic acid	2.892	$C_8H_8O_4$	$[M-H]^-$	167.035 1	4.2	122.991 1, 151.984 6	Yong (SDH)
19	Ajugol	3.201	$C_{15}H_{24}O_9$	$[M-H]^-$	347.135 2	2.9	113.025 9, 167.033 7, 181.050 6, 303.107 2	Yong (SDH)
20	Quinic acid	3.254	$C_7H_{12}O_6$	$[M-H]^-$	191.056 2	3.1	109.031 7, 127.040 7, 173.045 8, 191.056 7	Yong (WWZ)
21	5-Hydroxymethylfurfural	3.482	$C_6H_6O_3$	$[M+H]^+$	127.039 1	−3.1	109.030 8	Yong (MD, WWZ)
22	Neochlorogenic acid	5.040	$C_{16}H_{18}O_9$	$[M-H]^-$	353.087 8	1.4	127.033 0, 135.045 6, 161.027 9, 179.036 3, 191.057 4	Ti (XFH), Yong (DZY)
23	5-Hydroxymethyl-2-furaldehyde	5.163	$C_6H_6O_3$	$[M-H]^-$	125.023 6	−2.4	109.040 7	Yong (WWZ)
24	Decaffeoyl-verbascoside	5.237	$C_{20}H_{30}O_{12}$	$[M-H]^-$	461.164 9	−2.2	135.047 7, 123.041 9	Yong (SDH)
25	8-Epiloganic acid	5.630	$C_{16}H_{24}O_{10}$	$[M-H]^-$	375.128 9	−0.5	213.076 1, 169.088 4, 151.077 2	Yong (SDH)
26	Protocatechualdehyde	5.753	$C_7H_6O_3$	$[M-H]^-$	137.024 5	4.4	108.020 8, 109.025 7	Ti (XFH)
27	Acetylcatalpol	5.785	$C_{17}H_{24}O_{11}$	$[M-H]^-$	403.124 0	0.0	165.053 1, 139.039 6	Yong (SDH)
28	3,7-Dihydroxycoumarin	5.929	$C_9H_6O_4$	$[M-H]^-$	177.019 4	3.4	105.033 7, 133.028 4, 149.022 4	Ti (XFH)
29	Geniposide	6.239	$C_{17}H_{24}O_{10}$	$[M+Na]^+$	411.127 7	2.4	149.057 8, 103.048 8	Yong (SDH)
30	Schisandrol A	6.889	$C_{24}H_{32}O_7$	$[M+H]^+$	433.223 8	2.8	384.181 9, 353.161 3, 218.087 7	Yong (WWZ)
31	Cistanoside F	6.910	$C_{21}H_{28}O_{13}$	$[M-H]^-$	487.144 1	−2.3	179.033 5, 161.027 4, 135.046 9	Yong (SDH)
32	Caffeic acid	7.065	$C_9H_8O_4$	$[M-H]^-$	179.035 1	3.9	107.048 7, 109.029 8, 117.035 7, 134.039 4, 135.046 2, 136.084 1	Ti (XFH, ZGH), Yong (SDH)
33	Echinacoside	7.466	$C_{35}H_{46}O_{20}$	$[M+Na]^+$	809.247 1	−1.1	287.072 6, 163.038 7	Yong (SDH)
34	*sec*-Hydroxyaeginetic acid	7.860	$C_{15}H_{24}O_5$	$[M-H]^-$	283.155 7	4.2	163.107 6, 181.099 3, 203.162 4, 239.123 3, 265.127 2	Yong (SDH)
35	Cryptochlorogenic acid	7.962	$C_{16}H_{18}O_9$	$[M-H]^-$	353.088 2	2.5	111.048 6, 135.045 8, 155.036 4, 173.047 1, 179.037 1, 191.057 6	Ti (XFH), Yong (DZY)
36	Naringenin	8.263	$C_{15}H_{12}O_5$	$[M-H]^-$	271.061 7	4.1	151.004 3, 119.050 2	Yong (DZY))
37	5,7,4′-Trihydroxy-3′-methoxy-6,8-dimethyl-homisoflavanone	8.542	$C_{19}H_{20}O_6$	$[M+H]^+$	345.133 1	−2.0	137.053 3, 299.084 2	Yong (MD)
38	Liquiritin	8.562	$C_{21}H_{22}O_9$	$[M-H]^-$	417.118 4	−0.5	255.067 8, 161.024 0, 148.017 2	Ti (ZGC)
39	Chlorogenic acid	9.006	$C_{16}H_{18}O_9$	$[M-H]^-$	353.087 8	1.4	191.057 8, 179.036 5, 173.043 8	Ti (XFH), Yong (WWZ, DZY)
40	Prim-*O*-glucosylcimifugin	9.069	$C_{22}H_{28}O_{11}$	$[M+H]^+$	469.170 8	−0.4	235.060 4, 189.041 2	Yong (SDH)
41	Kaempferol-3-rutinoside	9.843	$C_{27}H_{30}O_{15}$	$[M+H]^+$	595.165 8	−0.8	415.089 1, 463.105 5	Ti (ZGC)
42	1,3-Dicaffeoylquinic acid	10.121	$C_{25}H_{24}O_{12}$	$[M-H]^-$	515.119 0	0.0	191.057 4, 179.036 2, 135.045 9	Ti (XFH)
43	Verbascoside	10.401	$C_{29}H_{36}O_{15}$	$[M+Na]^+$	647.196 0	1.2	501.139 9, 485.137 5, 339.090 7, 163.037 5	Yong (SDH)
44	Rutin	10.637	$C_{27}H_{30}O_{16}$	$[M+H]^+$	611.161 2	0.0	129.066 9, 257.068 3, 303.052 9, 465.106 9	Yong (DZY)
45	Neo-rehmannioside E	10.690	$C_{21}H_{34}O_{10}$	$[M-H]^-$	445.208 9	3.4	161.025 4, 265.099 2	Yong (SDH)
46	Isoschaftoside	11.052	$C_{26}H_{28}O_{14}$	$[M+H]^+$	565.154 9	−1.4	295.059 8, 325.071 0, 337.071 4, 391.081 7, 409.090 6, 427.100 8, 565.154 0	Ti (ZGC), Yong (DZY)

Continued

No.	Identification	t_R /min	Formula	Adducts	Precursor ion/*m*/*z*	Error /×10^6	Fragment ion/*m*/*z*	Origin plant
47	Schaftoside	11.062	$C_{26}H_{28}O_{14}$	$[M-H]^-$	563.139 5	−1.1	473.111 5, 383.078 5	Ti (ZGC)
48	Loliolid	11.123	$C_{11}H_{16}O_3$	$[M+H]^+$	197.117 8	0.0	105.075 8, 115.052 3, 133.099 6, 161.100 2, 179.103 5	Ti (XFH)
49	Quercetagetin-7-*O*-glucoside	11.207	$C_{21}H_{20}O_{13}$	$[M+H]^+$	481.097 0	−2.5	319.043 5	Ti (XFH)
50	5,7,2′-Trihydroxy-8-methyl-3-(3′,4′-methylenedioxybenzyl)-chromone	11.238	$C_{18}H_{14}O_7$	$[M+H]^+$	343.080 4	−4.1	205.046 7, 177.054 3, 149.056 7	Yong (MD)
51	Methyl eugenol	11.238	$C_{11}H_{14}O_2$	$[M+H]^+$	179.106 9	−1.7	117.062 9, 143.073 7, 144.080 6	Hua (XX)
52	Isoorientin	11.361	$C_{21}H_{20}O_{11}$	$[M+H]^+$	449.108 7	0.7	299.054 2, 166.021 8, 300.062 1	Yong (DZY)
53	Orientin	11.414	$C_{21}H_{20}O_{11}$	$[M-H]^-$	447.093 0	0.7	327.051 3, 357.064 0, 297.040 0	Yong (DZY)
54	Cistanoside A	11.671	$C_{36}H_{48}O_{20}$	$[M-H]^-$	799.263 7	−3.0	623.218 9, 175.037 8	Yong (SDH)
55	2-*O*-*β*-*D*-Glucopyranosyl atractyligenin	11.702	$C_{25}H_{38}O_9$	$[M-H]^-$	481.244 4	1.2	301.181 3, 320.184 0	Ti (XFH)
56	Rehmannioside C	11.723	$C_{19}H_{32}O_8$	$[M+Na]^+$	411.199 9	1.0	245.194 6	Yong (SDH)
57	Rehmapicroside	11.949	$C_{16}H_{26}O_8$	$[M-H]^-$	345.154 5	−1.2	165.054 5	Yong (SDH)
58	Liquiritigenin	12.156	$C_{15}H_{12}O_4$	$[M-H]^-$	255.066 0	1.2	135.048 0, 119.050 9	Ti (ZGC)
59	Liquiritin apioside	12.363	$C_{26}H_{30}O_{13}$	$[M-H]^-$	546.161 1	0.5	417.119 6, 255.067 4, 135.010 1	Ti (ZGC)
60	Afzelin	12.423	$C_{21}H_{20}O_{10}$	$[M-H]^-$	431.098 3	1.2	283.062 0, 311.056 1, 323.052 8	Ti (ZGC)
61	Isovitexin	12.434	$C_{21}H_{20}O_{10}$	$[M+H]^+$	433.113 4	−0.2	433.112 1, 313.072 1, 415.103 6	Yong (DZY)
62	Vitexin	12.444	$C_{21}H_{20}O_{10}$	$[M-H]^-$	431.097 0	−1.9	117.035 0, 283.061 1, 161.022 9	Yong (DZY)
63	Taxifolin	12.704	$C_{15}H_{12}O_7$	$[M-H]^-$	303.051 4	3.0	107.016 0, 125.026 2, 175.035 5, 217.054 2	Ti (XFH)
64	Quercetin-3-*O*-glucuronide	12.796	$C_{21}H_{18}O_{13}$	$[M+H]^+$	479.082 4	−0.4	303.048 9	Ti (XFH)
65	Quercetin	12.859	$C_{15}H_{10}O_7$	$[M-H]^-$	301.034 8	0.0	229.047 9, 178.997 2, 151.004 5	Ti (XFH), Yong (DZY)
66	Hyperoside	13.013	$C_{21}H_{20}O_{12}$	$[M-H]^-$	463.087 7	0.0	151.005 2, 255.031 6, 271.025 8, 300.028 1, 301.035 2	Ti (XFH)
67	Isoquercitrin	13.024	$C_{21}H_{20}O_{12}$	$[M-H]^-$	463.087 9	0.4	107.014 6, 151.004 6, 178.998 9, 255.029 7, 300.028 4, 301.033 9	Ti (XFH)
68	Patulitrin	13.231	$C_{22}H_{22}O_{13}$	$[M+H]^+$	495.114 1	0.4	318.035 9, 333.059 7	Ti (XFH)
69	Jiocarotenoside B1	13.415	$C_{37}H_{50}O_{20}$	$[M-H]^-$	813.280 3	−1.7	637.236 2, 175.032 2	Yong (SDH)
70	Azelaic acid	13.446	$C_9H_{16}O_4$	$[M-H]^-$	187.096 0	−5.3	125.095 4	Yong (MD)
71	Neo-rehmannioside B	13.633	$C_{15}H_{24}O_6$	$[M-H]^-$	299.149 3	−0.7	139.073 5	Yong (SDH)
72	Isorhamnetin-3-*O*-glucoside	13.675	$C_{22}H_{22}O_{12}$	$[M-H]^-$	477.103 7	0.8	107.021 1, 151.002 7, 285.040 5, 314.043 7, 315.051 7	Ti (XFH)
73	1,5-Dicaffeoylquinic acid	13.808	$C_{25}H_{24}O_{12}$	$[M-H]^-$	515.119 5	1.0	335.078 9, 191.056 4, 179.035 3	Ti (XFH)
74	Forsythoside A	14.026	$C_{29}H_{36}O_{15}$	$[M-H]^-$	623.198 1	0.8	177.017 3, 119.048 2	Yong (SDH)
75	Isochlorogenic acid A	15.214	$C_{25}H_{24}O_{12}$	$[M-H]^-$	515.119 5	1.0	203.037 2, 191.057 1, 179.036 2	Ti (XFH)
76	5-Methoxy-6-methyl-7-oxhydryl-8-methoxy-3-(2′-oxhydryl-4′-methoxybenzyl)-4-chromanone	15.429	$C_{20}H_{22}O_7$	$[M-H]^-$	373.129 8	2.9	153.019 6, 168.046 0	Yong (MD)
77	5,7-Dihydroxy-3-(4′-methoxybenzyl)-4-chromone	15.865	$C_{17}H_{14}O_5$	$[M-H]^-$	297.075 2	−3.7	203.037 1, 175.046 9	Yong (MD)
78	Aegineticacid	15.957	$C_{15}H_{24}O_4$	$[M+H]^+$	269.176 4	4.1	167.010 4	Yong (SDH)
79	Formononetin	16.122	$C_{16}H_{11}O_4$	$[M-H]^-$	267.066 0	1.1	252.044 8	Ti (ZGC)
80	Ophiopogonanone E	16.308	$C_{19}H_{20}O_7$	$[M-H]^-$	359.113 6	1.4	208.034 1, 138.035 6	Yong (MD)
81	5,7-Dihydroxy-6,8-dimethyl-3-(3′,5′-dimethoxy-4′-hydroxybenzyl)-4-chromanone	16.339	$C_{20}H_{22}O_7$	$[M-H]^-$	373.130 0	3.5	207.064 6, 179.070 1, 135.046 6	Yong (MD)
82	5,7-Dihydroxy-8-methyl-3-(3′,4′-dimethoxybenzyl)-4-chromone	16.410	$C_{18}H_{14}O_6$	$[M-H]^-$	325.071 8	1.8	297.073 3, 131.053 8, 203.035 9	Yong (MD)
83	Neoliquiritin	16.474	$C_{21}H_{22}O_9$	$[M+H]^+$	419.132 6	−3.8	119.047 6, 137.022 1, 239.069 7, 257.080 6	Ti (ZGC)
84	Isoliquiritin	16.959	$C_{21}H_{22}O_9$	$[M+H]^+$	419.135 1	2.1	137.023 2, 239.070 8, 257.082 5	Ti (ZGC)
85	Isoliquiritigenin	16.969	$C_{15}H_{12}O_4$	$[M+H]^+$	257.081 0	−1.6	137.023 8	Ti (ZGC)
86	Martynoside	17.103	$C_{31}H_{40}O_{15}$	$[M-H]^-$	651.228 5	−0.6	193.048 0, 175.042 1	Yong (SDH)
87	Spinacetin	17.216	$C_{17}H_{14}O_8$	$[M-H]^-$	345.061 6	1.7	315.014 5, 330.038 3	Ti (XFH)

Continued

No.	Identification	t_R /min	Formula	Adducts	Precursor ion/*m*/*z*	Error /×10^6	Fragment ion/*m*/*z*	Origin plant
88	5-Oxhydryl-6-methyl-7-methoxy-3-(3′,4′-dihydroxyphenyl)-4-chromone	17.546	$C_{18}H_{16}O_6$	$[M-H]^-$	327.086 5	−1.2	164.049 8, 327.084 9	Yong (MD)
89	Uralsaponin F	17.693	$C_{44}H_{64}O_{19}$	$[M-H]^-$	895.399 4	3.4	853.394 4, 821.353 5, 351.059 5	Ti (ZGC)
90	1-*O*-Acetyl britannilactone	18.354	$C_{17}H_{24}O_5$	$[M+H]^+$	309.169 2	−3.2	291.050 0, 231.136 9, 203.141 2	Ti (XFH)
91	Luteolin	18.404	$C_{15}H_{10}O_6$	$[M-H]^-$	285.039 7	−0.7	175.035 6, 151.004 5, 133.026 6	Ti (XFH), Yong (DZY)
92	Eupafolin	18.684	$C_{16}H_{12}O_7$	$[M-H]^-$	315.051 3	2.5	300.027 4	Ti (XFH)
93	Rosmarinic acid	20.563	$C_{18}H_{16}O_8$	$[M-H]^-$	359.077 4	1.9	133.029 3, 135.044 2, 161.025 6, 193.014 4	Ti (XFH)
94	Licorice saponin A3	20.770	$C_{48}H_{72}O_{21}$	$[M+H]^+$	985.467 6	3.2	453.336 4, 471.348 0, 615.389 4, 809.433 9	Ti (ZGC)
95	Diosmetin	21.069	$C_{16}H_{12}O_6$	$[M-H]^-$	299.056 9	4.3	227.037 1, 256.039 1, 284.032 8	Yong (DZY)
96	Ophiopogonin D	21.070	$C_{44}H_{70}O_{16}$	$[M+H]^+$	855.471 6	−3.0	251.178 2, 287.200 7, 431.313 8, 559.363 5, 577.379 1, 711.368 9, 723.434 0	Yong (MD)
97	Licorice saponin G2	21.153	$C_{42}H_{62}O_{17}$	$[M+H]^+$	839.408 6	2.5	451.320 7, 469.331 2, 487.341 5, 663.377 1	Ti (ZGC)
98	Licorice saponin E2	21.193	$C_{42}H_{60}O_{16}$	$[M+H]^+$	821.395 8	−0.2	451.323 1, 469.332 6, 645.364 4	Ti (ZGC)
99	Gancaonin G	21.203	$C_{21}H_{20}O_5$	$[M+H]^+$	353.139 8	2.5	267.063 7, 297.108 2	Ti (ZGC)
100	Glycyrrhetinic acid	21.266	$C_{30}H_{46}O_4$	$[M+H]^+$	471.346 2	−2.5	407.329 5, 435.326 9, 453.337 0	Ti (ZGC)
101	Neobritannilactone B	21.276	$C_{15}H_{20}O_3$	$[M-H]^-$	247.133 8	1.6	203.148 3, 201.132 8, 135.083 1	Ti (XFH)
102	Methylophiopogonone A	21.286	$C_{19}H_{16}O_6$	$[M-H]^-$	339.087 3	1.2	311.093 4, 217.208 3	Yong (MD)
103	Ophiopogonanone B	21.328	$C_{19}H_{20}O_5$	$[M-H]^-$	327.124 5	4.0	178.066 9	Yong (MD)
104	Glycyrrhizic acid	21.389	$C_{42}H_{62}O_{16}$	$[M-H]^-$	821.396 3	0.4	351.055 0, 193.034 8, 469.344 7	Ti (ZGC)
105	Pregomisin	21.431	$C_{22}H_{30}O_6$	$[M+H]^+$	391.212 2	0.3	327.143 6, 275.084 7, 229.096 2	Yong (WWZ)
106	Uralsaponin C	21.473	$C_{42}H_{64}O_{16}$	$[M+H]^+$	825.428 1	1.0	455.351 0, 473.361 4	Ti (ZGC)
107	8-Formyl ophiopogonone B	21.534	$C_{20}H_{22}O_7$	$[M+H]^+$	375.143 9	−1.3	109.062 1, 251.090 2, 357.133 8	Yong (MD)
108	Casticin	21.699	$C_{19}H_{18}O_8$	$[M+H]^+$	375.107 6	−1.1	360.082 6, 375.103 9, 377.116 6	Ti (XFH)
109	Schisandrol B	21.751	$C_{23}H_{28}O_7$	$[M+H]^+$	417.192 3	2.4	368.147 1, 399.179 9	Yong (WWZ)
110	Diosgenin	21.804	$C_{27}H_{42}O_3$	$[M+H]^+$	415.321 5	0.7	157.095 5	Yong (MD)
111	Ilicic acid	21.824	$C_{15}H_{24}O_3$	$[M-H]^-$	251.165 8	4.4	207.173 2	Ti (XFH)
112	Japonicones D	21.885	$C_{34}H_{44}O_9$	$[M+H]^+$	597.305 9	−0.8	211.109 5, 185.132 0	Ti (XFH)
113	Gomisin D	21.896	$C_{28}H_{34}O_{10}$	$[M+H]^+$	531.224 5	2.8	401.158 9, 383.149 2, 341.101 3	Yong (WWZ)
114	Gomisin R	21.906	$C_{22}H_{24}O_7$	$[M+H]^+$	401.159 3	−1.7	337.106 6, 341.102 8, 383.148 2	Yong (WWZ)
115	Gomisin J	21.927	$C_{22}H_{28}O_6$	$[M+H]^+$	389.194 5	−4.9	227.075 0, 287.092 0, 137.060 1	Yong (WWZ)
116	5-Oxhydryl-6-aldehyde-7-methoxy-8-methyl-3-(4′-methoxybenzyl)-4-chromanone	21.937	$C_{20}H_{20}O_6$	$[M-H]^-$	355.120 0	5.1	217.052 1, 150.031 8	Yong (MD)
117	Ruscogenin	21.938	$C_{27}H_{42}O_4$	$[M+H]^+$	431.316 8	1.6	251.177 6, 269.185 4, 139.078 6	Yong (MD)
118	Sesamin	21.959	$C_{20}H_{18}O_6$	$[M+H]^+$	355.117 9	−0.8	179.035 7, 268.985 4	Hua (XX)
119	Angeloylgomisin H	22.029	$C_{28}H_{36}O_8$	$[M+H]^+$	501.248 9	0.2	370.173 1, 355.154 4, 337.142 4	Yong (WWZ)
120	Schisantherin B	22.071	$C_{28}H_{34}O_9$	$[M+H]^+$	515.227 9	−0.4	385.165 4, 355.152 5, 343.116 8	Yong (WWZ)
121	Benzoylgomisin H	22.155	$C_{30}H_{34}O_8$	$[M+H]^+$	523.231 3	−3.6	441.181 5, 409.159 0, 386.174 3	Yong (WWZ)
122	Gedunin	22.155	$C_{28}H_{34}O_7$	$[M+H]^+$	483.238 3	0.0	381.133 3, 395.149 1, 367.117 2	Yong (WWZ)
123	Schisandrin B	22.155	$C_{23}H_{28}O_6$	$[M+H]^+$	401.195 8	−1.5	386.174 3, 370.177 3	Yong (WWZ)
124	Alantolactone	22.195	$C_{15}H_{20}O_2$	$[M+H]^+$	233.153 9	1.7	159.114 6, 118.071 1, 106.073 7	Ti (XFH)
125	Schisanhenol B	22.237	$C_{22}H_{26}O_6$	$[M+H]^+$	387.179 7	−2.8	355.154 1, 326.150 7, 271.060 4	Yong (WWZ)
126	Schisandrin C	22.350	$C_{22}H_{24}O_6$	$[M+H]^+$	385.166 2	2.9	257.080 8, 199.074 8, 184.051 5	Yong (WWZ)
127	Schisantherin A	22.381	$C_{30}H_{32}O_9$	$[M+H]^+$	537.209 6	−5.4	415.173 3, 397.163 7, 371.148 9	Yong (WWZ)
128	Schisandrin A	22.753	$C_{24}H_{32}O_6$	$[M+H]^+$	417.226 5	−2.9	402.203 2, 386.204 3, 371.184 9	Yong (WWZ)
129	Schisanhenol	22.504	$C_{23}H_{30}O_6$	$[M+H]^+$	403.211 0	−2.7	302.116 8, 271.093 8	Yong (WWZ)
130	Asarinin	22.940	$C_{20}H_{18}O_6$	$[M+NH_4]^+$	372.144 4	−0.8	128.060 9, 135.038 8, 161.063 1	Hua (XX)
131	5,7,2′-Trihydroxy-6,8-dimethyl-3-(3′,4′-methylenedioxybenzyl)-chromone	22.961	$C_{19}H_{16}O_7$	$[M+H]^+$	357.097 2	−0.6	339.097 9	Yong (WWZ)
132	Dibutyl phthalate	23.239	$C_{16}H_{22}O_4$	$[M+H]^+$	279.160 9	4.7	149.022 3, 121.027 8	Yong (WWZ)

及文献[19]报道, 推测该化合物为五味子甲素, 其可能的裂解方式见图2A。

1.2.2　苯乙醇苷类化合物的鉴定　化合物43在正离子模式下检出, 保留时间为10.401 min, 准分子离子峰为*m/z* 647.196 0 [M+Na]$^+$, 推测化学式为$C_{29}H_{36}O_{15}$。其裂解途径有2条, 途径一是裂解时脱去咖啡酰基$C_9H_7O_3$生成*m/z* 485.137 5 [M+Na−Caffeoyl]$^+$, 后又脱去$C_6H_{10}O_5$生成*m/z* 339.090 7 [M+Na−Caffeoyl−$C_6H_{10}O_5$]$^+$; 途径二是糖苷键断裂后脱去一分子鼠李糖生成*m/z* 501.139 9 [M+Na−Rha]$^+$, 后脱去咖啡酰基生成*m/z* 339.090 7 [M+Na−Rha−Caffeoyl]$^+$, *m/z* 163.037 5 [M+Na−$C_{20}H_{28}O_{12}$]$^+$为其脱去的咖啡酰基, 结合数据库及文献[20]报道, 推测该化合物为毛蕊花糖苷, 其可能的裂解方式见图2B。

1.2.3　黄酮类化合物的鉴定　化合物44在正离子模

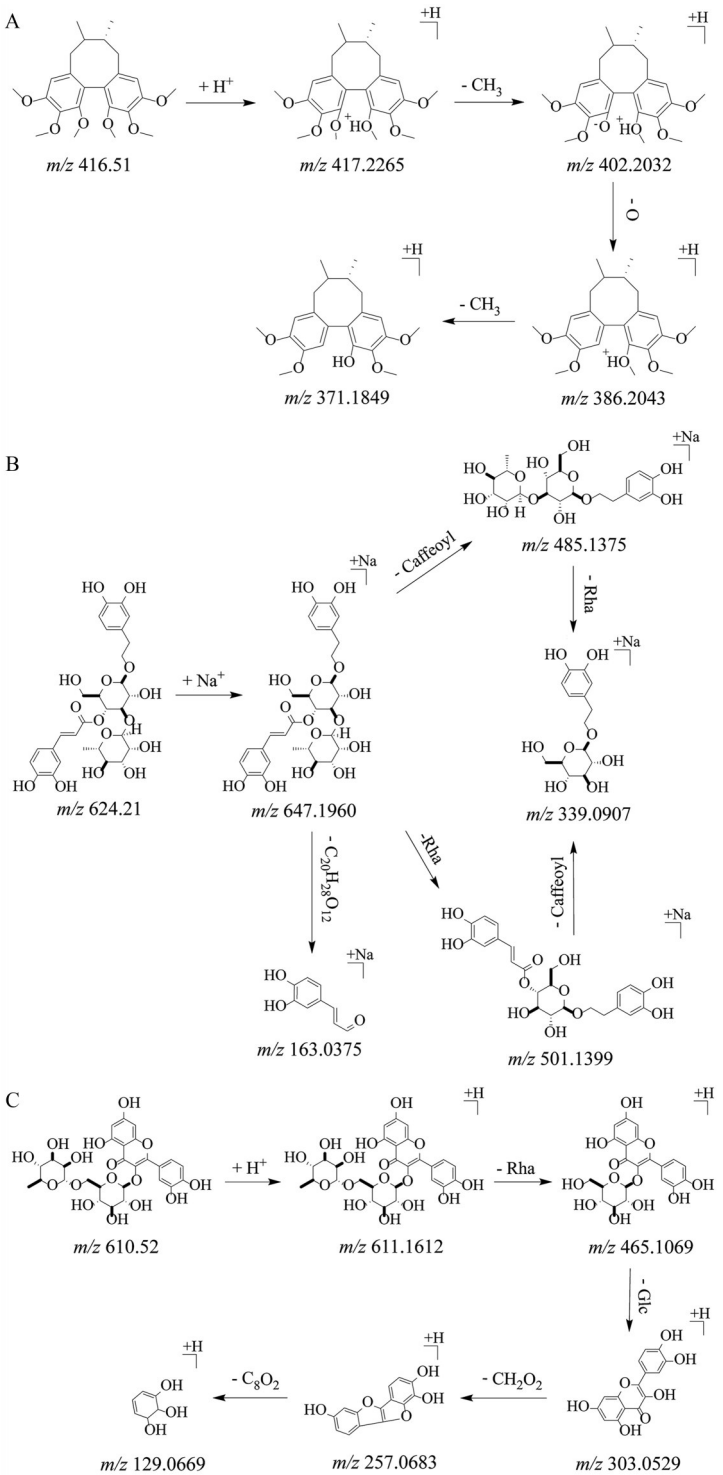


Figure 2　Mass spectrometry fragmentation pathways. A: Schisandrin A; B: Verbascoside; C: Rutin

式下检出, 保留时间为10.637 min, 准分子离子峰为*m/z* 611.161 2 $[M+H]^+$, 推测化学式为$C_{27}H_{30}O_{16}$。裂解时脱去一分子鼠李糖生成*m/z* 465.106 9 $[M+H-Rha]^+$, 后又脱去一分子葡萄糖生成*m/z* 303.052 9 $[M+H-Rha-Glc]^+$, 在碎片离子*m/z* 303.052 9 $[M+H-Rha-Glc]^+$中丢失A环上一分子H_2O和C环上CO形成*m/z* 257.068 3 $[M+H-Rha-Glc-H_2O-CO]^+$, 丢失A环和C环并发生重排后形成*m/z* 129.066 9 $[M+H-Rha-Glc-CH_2O_2-C_8O_2]^+$, 结合数据库和文献[21]报道, 推测该化合物为芦丁, 其可能的裂解方式见图2C。

1.2.4 甾体皂苷类化合物的鉴定 化合物96在正离子模式下检出, 保留时间为21.070 min, 准分子离子峰为*m/z* 855.471 6 $[M+H]^+$, 推测化学式为$C_{44}H_{70}O_{16}$。其主要裂解途径有3条, 途径一是连续丢失糖基, 丢失木糖后生成*m/z* 723.434 0 $[M+H-Xyl]^+$, 后失去一分子鼠李糖生成*m/z* 577.379 1 $[M+H-Xyl-Rha]^+$, 脱去一分子H_2O生成*m/z* 559.363 5 $[M+H-Xyl-Rha-H_2O]^+$; 途径二是糖苷键断裂, 丢失一分子木糖、一分子鼠李糖和一分子岩藻糖, 生成*m/z* 431.313 8 $[M+H-Xyl-Rha-Fuc]^+$, 继而中性丢失$C_8H_{16}O_2$生成*m/z* 287.200 7 $[M+H-Xyl-Rha-Fuc-C_8H_{16}O_2]^+$, 再丢失两分子$H_2O$生成*m/z* 251.178 2 $[M+H-Xyl-Rha-Fuc-C_8H_{16}O_2-2H_2O]^+$; 途径三是首先特征中性丢失$C_8H_{16}O_2$生成*m/z* 711.362 8 $[M+H-C_8H_{16}O_2]^+$, 后糖苷键断裂生成*m/z* 287.200 7 $[M+H-C_8H_{16}O_2-Xyl-Rha-Fuc]^+$, 后又丢失两分子$H_2O$生成*m/z* 251.178 2 $[M+H-C_8H_{16}O_2-Xyl-Rha-Fuc-2H_2O]^+$, 根据数据库及文献[22]报道, 推测该化合物为麦冬皂苷D, 其可能裂解方式见图3A。

1.2.5 环烯醚萜类化合物的鉴定 化合物12在负离子模式下检出, 保留时间为1.693 min, 准分子离子峰为*m/z* 685.219 8 $[M-H]^-$, 推测化学式为$C_{27}H_{42}O_{20}$。裂解时丢失一分子H_2O和一分子葡萄糖生成*m/z* 505.149 9 $[M-H-Glc-H_2O]^-$, 后糖苷键断裂, 母核上中性丢失$C_9H_8O_3$生成*m/z* 341.112 9 $[M-H-Glc-H_2O-C_9H_8O_3]^-$, 再丢失一分子$C_2H_6O_3$生成*m/z* 263.077 6 $[M-H-Glc-H_2O-C_9H_8O_3-C_2H_6O_3]^-$, 或者在*m/z* 341.112 9 $[M-H-Glc-H_2O-C_9H_8O_3]^-$碎片离子上糖苷键断裂, 失去一分子葡萄糖生成*m/z* 179.055 3 $[M-H-Glc-H_2O-C_9H_8O_3-Glc]^-$, 结合数据库和文献[23]报道, 推测该化合物为地黄苷D, 其可能裂解方式见图3B。

1.2.6 倍半萜内酯类化合物的鉴定 化合物90在正离子模式下检出, 保留时间为18.354 min, 准分子离子峰为*m/z* 309.169 2 $[M+H]^+$, 推测化学式为$C_{17}H_{24}O_5$。裂解时失去一分子H_2O生成*m/z* 291.050 0 $[M+H-H_2O]^+$, 后丢失一分子$C_2H_4O_2$生成*m/z* 231.136 9 $[M+H-H_2O-C_2H_4O_2]^+$, 再脱去一分子CO生成*m/z* 203.141 2 $[M+H-H_2O-C_2H_4O_2-CO]^+$, 结合数据库和文献[24]报道, 推测该化合物为1-*O*-乙酰旋覆花内酯, 其可能裂解方式见图3C。

1.3 大补肺汤含量测定

取大补肺汤水提液, 配制成供试品溶液, 并测定其中7个成分的含量, 测定结果见表4。

2 大补肺汤网络药理学分析

2.1 大补肺汤潜在活性成分及作用靶点

大补肺汤体组、用组、化组分别收集到32、51、6个潜在活性成分, 其中体组和用组具有5个相同成分。体组、用组、化组分别获得508、679、138个作用靶点, 其中体组和用组作用于326个相同靶点, 体组和化组作用于15个相同靶点, 用组和化组作用于7个相同靶点, 体组、用组、化组共同作用于79个靶点。

2.2 大补肺汤及体−用−化各组潜在活性成分−COPD稳定期靶点网络构建与聚类分析

如图4所示, 共收集到2 142个与COPD稳定期相关的靶点, 其与大补肺汤有294个共同靶点, 与体组有212个共同靶点, 与用组有256个共同靶点, 与化组有55个共同靶点。对共同靶点进行PPI网络的构建与筛选后, 利用Cytoscape构建大补肺汤潜在活性成分-COPD稳定期靶点网络。其中, 根据度值排名前十的活性成分为槲皮素、五味子醇乙、五味子甲素、五味子丙素、甲基麦冬黄烷酮A、甲基麦冬黄酮A、麦冬黄烷酮A、1-*O*-乙酰旋覆花内酯、大花旋覆花素、甘草宁E, 推测可能为大补肺汤治疗COPD稳定期的核心成分。

如图5所示, 将大补肺汤治疗COPD稳定期的潜在靶点输入STRING数据库获得蛋白间相互作用关系, 导入Cytoscape软件并构建PPI网络图, 选取度值、BC、CC均为均值以上的靶点作为核心靶点, 得到STAT3、SRC、HSP90AA1、PIK3R1、PIK3CA、PIK3CB、PIK3CD、AKT1、ESR1、EGFR等87个核心靶点。将筛选得到的靶点导入Metascape数据库中进行GO生物功能富集分析和KEGG通路富集分析, GO功能富集分析得到3 223个条目, 提示大补肺汤治疗COPD稳定期主要以细胞迁移调控、信号转导、磷酸化作用为主的生物过程 (BP), 以膜微区、激酶复合物、胞质与囊泡为主的细胞组分 (CC) 和以激酶活性、激酶结合为主的分子功能 (MF); KEGG信号通路分析结果表明大补肺汤治疗COPD稳定期可能与PI3K-AKT信号通路、HIF-1α信号通路、AGE-RAGE信号通路、EGFR酪氨酸激酶抑制剂耐药性、MAPK信号通路等相关。

分别对大补肺汤的体、用、化各组进行PPI网络的构建和GO生物功能富集分析及KEGG通路富集分析, 结果如图6所示。“体组”筛选得到STAT3、SRC、HSP90AA1、PIK3CA、PIK3CB等核心靶点, GO功能富

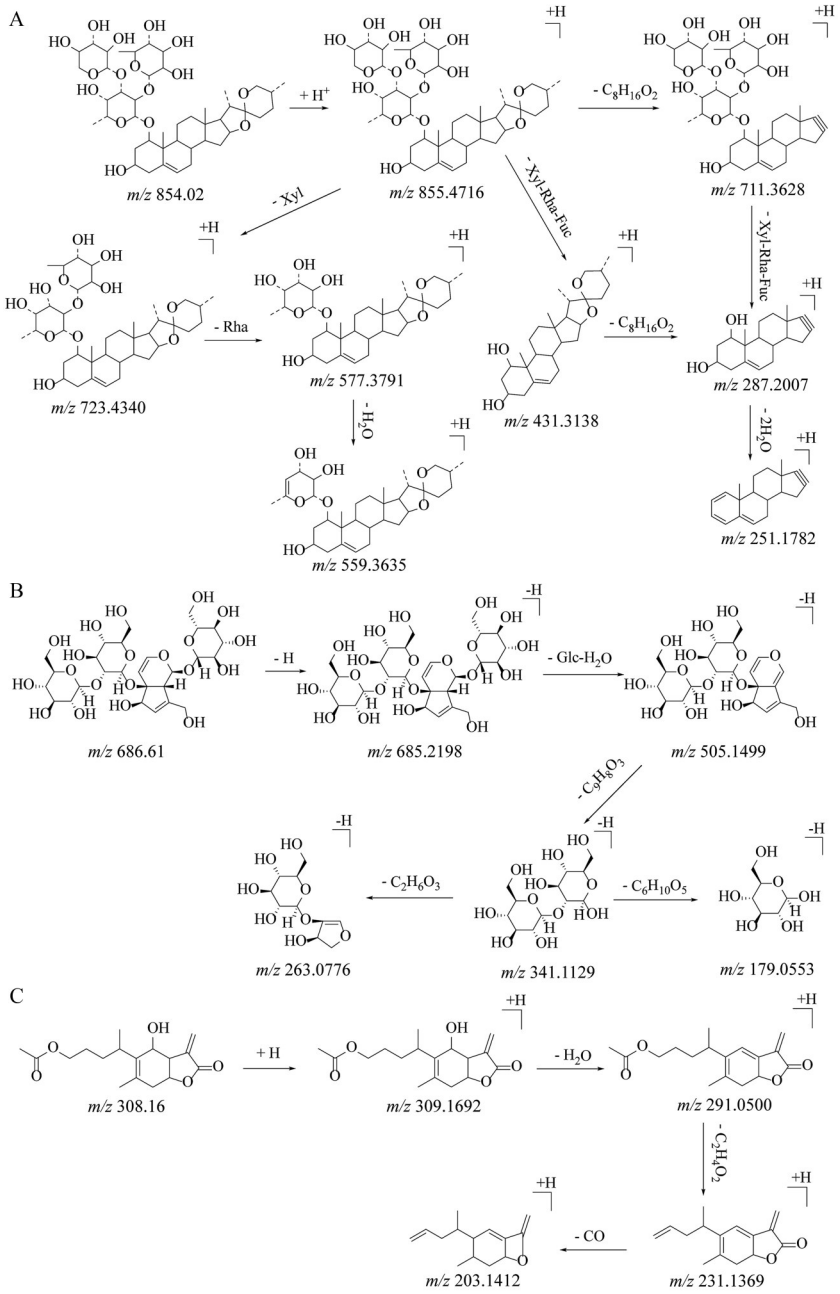


Figure 3　Mass spectrometry fragmentation pathways. A: Ophiopogonin D; B: Rehmannioside D; C: 1-*O*-Acetyl britannilactone

Table 4　Contents of 7 active components in DBFT (n = 3)

Component	Content/mg·g^{-1}
Schisandrol B	0.93 ± 0.04
Schizandrin A	0.37 ± 0.07
Schisandrin C	1.15 ± 0.11
Methylophiopogonone A	2.62 ± 0.31
Ophiogonanone A	3.00 ± 0.23
1-*O*-Acetyl britannilactone	2.37 ± 0.06
Britannin	0.73 ± 0.13

集分析得到2 736个条目, 主要以信号转导、细胞迁移、腺体发育为主的生物过程, 以质膜、胞内囊泡为主的细胞组分和以蛋白相互作用、激酶活性、蛋白质磷酸化修饰为主的分子功能; KEGG信号通路分析结果表明体组可能与PI3K-AKT信号通路、HIF-1α信号通路、C型凝集素受体信号通路、Th17细胞的分化过程、FoxO信号通路等相关。“用组”筛选得到STAT3、SRC、PIK3R1、HSP90AA1、PIK3CA等核心靶点, GO功能富集分析得到3 034个条目, 主要以细胞运动与迁移、磷酸化作用、对外部刺激和细胞因子的响应为主的生物过程, 以膜微区、激酶复合物为主的细胞组分和以蛋白激酶活性、蛋白相互作用为主的分子功能; KEGG信号通路分析结果表明用组可能与PI3K-AKT信号通路、AGE-RAGE信号通路、HIF-1α信号通路、Ras信号通路等相关。“化组”

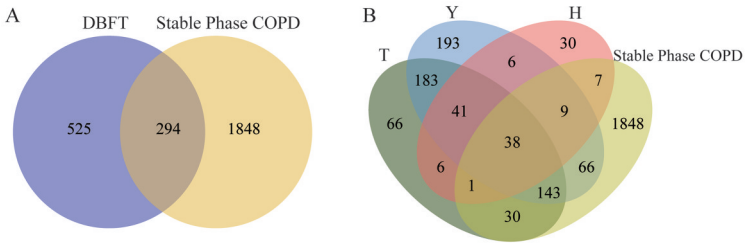


Figure 4 Venn diagram of common targets among DBFT and the stable phase COPD. COPD: Chronic obstructive pulmonary disease; A: DBFT; B: "Ti-Yong-Hua" groups

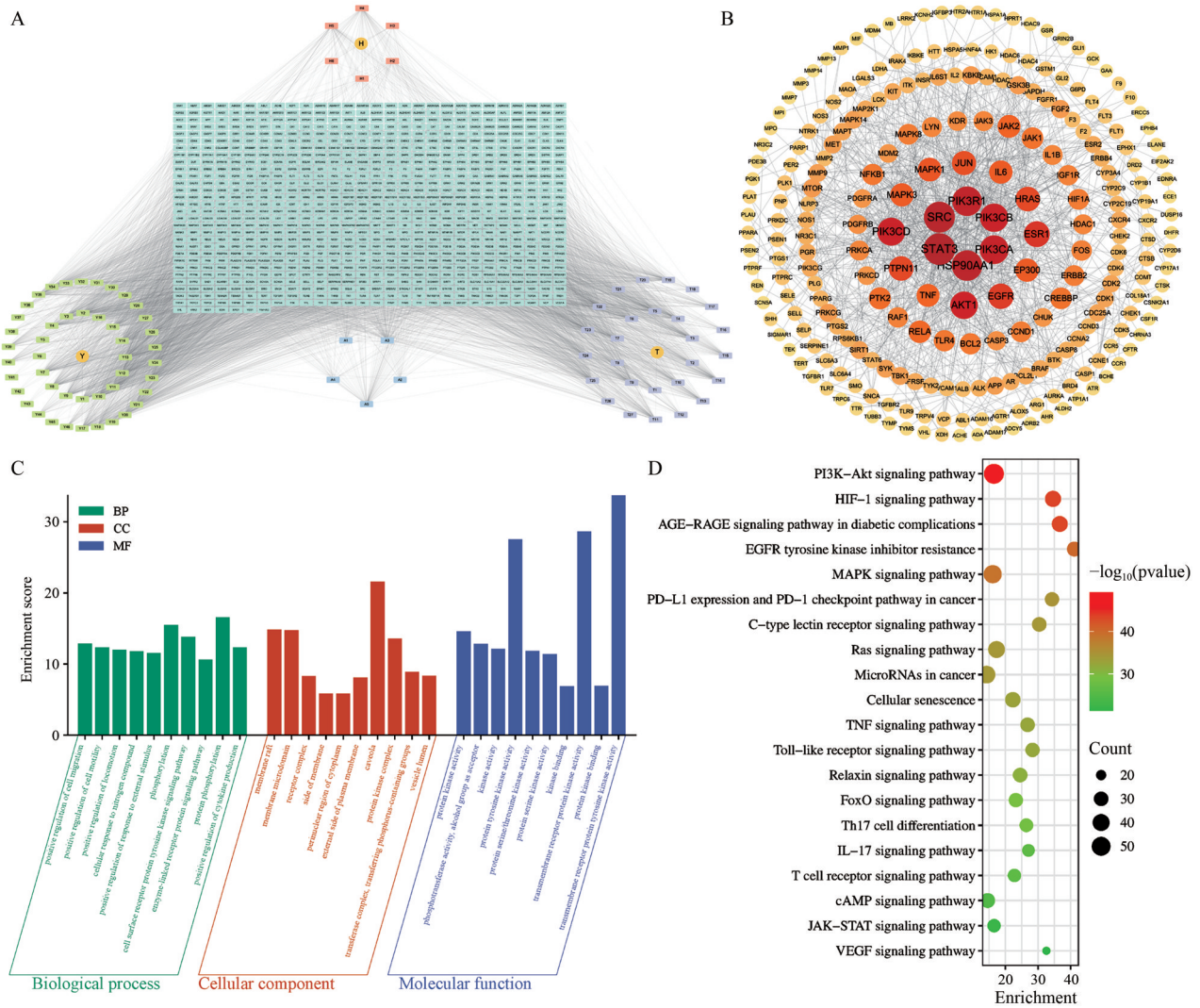


Figure 5 Construction and enrichment analysis of the potential active component-stable phase COPD target network of DBFT. A: Compound-target network; B: Protein-protein interaction network; C: GO functional enrichment analysis; D: KEGG pathway enrichment analysis

筛选得到HSP90AA1、JAK2、JAK1、CREBBP、PIK3CB等核心靶点, GO功能富集分析得到980个条目, 主要以磷酸化作用、氧化应激作用、蛋白质核定位调控为主的生物过程, 以膜微区、神经元为主的细胞组分和以激酶活性、组蛋白表观调控为主的分子功能; KEGG信号通路分析结果表明化组可能与Th17细胞的分化过程、PI3K-AKT信号通路、Toll样受体信号通路、FoxO信号通路、细胞凋亡、Th1和Th2细胞分化等通路相关。通过物质基础分析得知, 用于治疗COPD稳定期的化学成分主要为用组的成分, 这为该方体−用−化配伍机制研究提供了依据和参考。

讨论

根据《辅行诀脏腑用药法要》中的记载, 大补肺汤

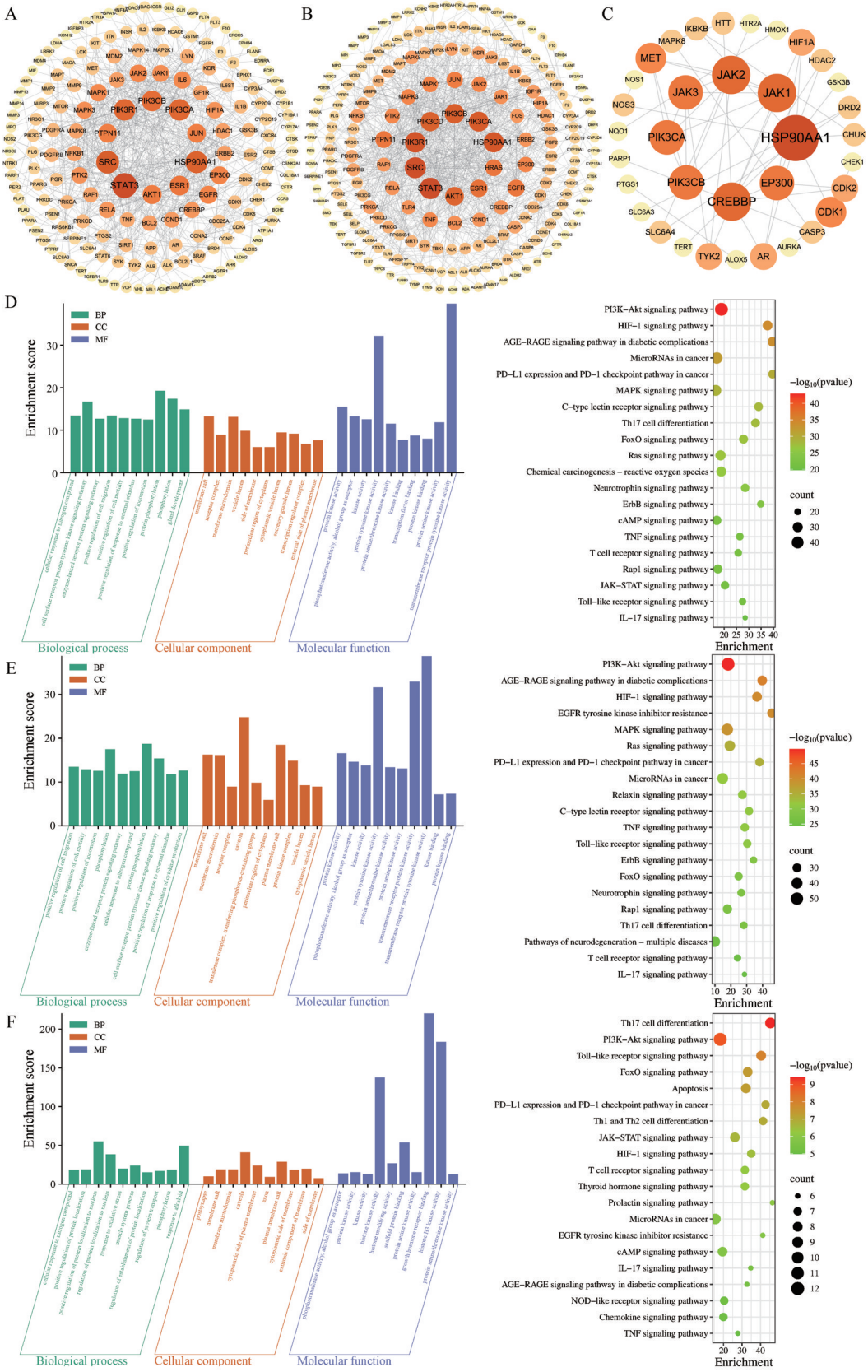


Figure 6　Construction and enrichment analysis of targets between "Ti-Yong-Hua" groups of DBFT and stable phase COPD. A: Protein-protein interaction network of Ti; B: Protein-protein interaction network of Yong; C: Protein-protein interaction network of Hua; D: GO functional and KEGG pathway enrichment analysis of Ti; E: GO functional and KEGG pathway enrichment analysis of Yong; F: GO functional and KEGG pathway enrichment analysis of Hua

主治烦热汗出, 少气不足息, 口干, 耳聋, 脉虚而快等症, 可用于治疗肺肾两虚, 肃降无权所致的肺虚疾病中的“肺肾气阴两虚证”, 其功效为补益肺肾、纳气平喘, 在临床上已用于治疗COPD稳定期。全方由五味子、麦冬、生地黄、淡竹叶、旋覆花、炙甘草、细辛七味药组成, 麦门冬养阴润肺以通脉道、以除烦热; 五味子收降阴津、纳气平喘; 旋覆花降气消痰; 细辛宣肺止咳, 且细辛之辛开与五味子之酸敛, 一开一合, 开阖肺气, 化痰而不伤正; 地黄滋阴补肾, 竹叶除烦生津, 二者合用助肾水清降火热; 甘草助肾体, 助地黄益肾水以滋泽其肺燥, 甘草与旋覆花同用, 乃咸甘除燥之法, 使痰涎去而津液复。但大补肺汤的成分复杂, 治疗COPD稳定期的药效物质基础尚未明确, 不利于其临床应用与更为深入的研究。本实验分析了大补肺汤的化学成分, 结合网络药理学探讨大补肺汤治疗COPD稳定期的作用靶点, 并分别分析了体、用、化各组的作用靶点, 为大补肺汤的后续研究和临床应用提供数据支持。

通过UPLC-Q-TOF-MS/MS技术鉴定出132种化学成分, 并结合网络药理学筛选出槲皮素、五味子醇乙、五味子甲素、五味子丙素、甲基麦冬黄烷酮A、甲基麦冬黄酮A、麦冬黄烷酮A、1-*O*-乙酰旋覆花内酯、大花旋覆花素、甘草宁E等活性成分, 前10种核心成分7种来自用组, 4种来自体组, 槲皮素为体组、用组共有成分, 这与《辅行诀》中治疗COPD稳定期等肺虚之证采用补用为主、泻体为辅的治法相对应。其中槲皮素可以通过抑制Wnt5a/β-catenin信号通路、自噬过度和氧化应激, 从而减轻ASMC的线粒体损伤和表型转换, 在COPD中显示出潜在的治疗作用[25]; 五味子甲素可以通过抑制α-SMA的表达的TGF-β信号通路在小鼠体内减弱BLM诱导的胶原沉积, 从而减轻小鼠肺纤维化的程度[26]; 1-*O*-乙酰旋覆花内酯通过调节SRC/EGFR/MAPK信号通路抑制MUC5AC的表达并发挥抗炎作用, 在COPD小鼠体内显著抑制气管炎性细胞浸润和黏液分泌过多[27]; 甘草宁E抑制了LPS诱导的RAW264.7细胞中NO和PGE2的产生, 显著降低了LPS诱导的A549细胞中COX-2和促炎细胞因子的表达, 通过抑制MAPK和NF-κB信号通路来缓解炎症反应, 可用于治疗肺部的炎症[28]。

PPI分析结果显示大补肺汤与COPD稳定期相关联的核心靶点为STAT3、SRC、HSP90AA1、PIK3R1、PIK3CA、PIK3CB、PIK3CD、AKT1、ESR1、EGFR等, 这些靶点大多与细胞存活、细胞增殖、细胞代谢、炎症和免疫抑制等有关。STAT3是JAK2的下游靶点, 参与粒细胞生成过程中的中性粒细胞分化, STAT3抑制剂的使用显著降低了PPE诱导的小鼠肺部Siglec-F$^+$中性粒细胞的数量, 显著缓解了小鼠肺气肿的症状, 同时还大幅减少了常规中性粒细胞的数量, 这反映了STAT3在Siglec-F$^+$中性粒细胞分化和IL-17表达中的广泛应用, STAT3抑制可能通过抑制IL-17/CXCL-1轴, 从而减轻了中性粒细胞向肺部的整体迁移[29,30]; SRC家族激酶参与LPS和氧化应激对巨噬细胞的激活[31], 香烟烟雾会激活SRC, 促进气道炎症和肺组织的破坏, PM2.5暴露会激活BEAS-2B细胞中SRC蛋白激酶的激活, 引起气道炎症, 引发支气管炎、哮喘和慢阻肺等疾病; PIK3CA、PIK3CB、PIK3CD是PI3K的催化亚基, PIK3R1是PI3K的调节亚基, PI3K通过促进炎症、氧化应激和组织重塑, 在COPD中发挥关键作用, 导致疾病的进展和恶化, PI3K抑制剂可以减少炎症并增强免疫调节, 防止血管重塑和纤维化[32,33]。其中体组、用组共同作用于PI3K各亚基、STAT3和SRC, 直接抑制了炎症的进一步发展, 并且通过调控细胞的生存状态, 阻止细胞在外界刺激下异常存活和增殖, 减缓气道重塑和肺气肿的进程。化组聚焦于JAK1和JAK2, 此为细胞因子 (如白细胞介素、干扰素) 受体的关键激酶, 影响STAT3的表达, 从更深层次地调控了大补肺汤在治疗COPD稳定期时的抗炎通路。EGFR在COPD病程中的黏液高分泌和气道纤维化重塑起到了重要作用, 研究表明, IL-33激活RAGE/EGFR通路导致黏液相关基因的表达途径, 导致上皮细胞重塑过度、黏蛋白分泌过多、纤毛功能异常, 增加COPD病程恶化的风险, 大补肺汤体−用−化三组联用后可以调控EGFR的表达, 从而减轻COPD炎症的发生和气道阻塞程度[34]。

慢阻肺的发病机制普遍认为与炎症、氧化应激、蛋白酶/抗蛋白酶失衡和免疫力下降有关。吸烟、PM2.5等诱导的氧化应激和蛋白酶过度生成是COPD发病的主要因素, 导致肺泡细胞死亡、肺泡细胞外基质破坏和肺泡结构丧失, 在呼吸道上主要表现为肺泡间隙扩大、气道重塑和黏液潴留, 进而导致肺功能的下降, 这涉及多种炎症细胞、炎性介质和相关信号通路[35]。大补肺汤的体、用、化三组均可作用于PI3K-AKT信号通路, 该信号通路的激活可通过炎症和氧化应激来加剧COPD的进展[36]。研究表明PI3K-AKT信号通路在COPD小鼠的肺泡巨噬细胞中被激活, 促使TNF-α、IL-1β、IL-6等促炎因子显著增加, 且促进了COPD小鼠肺部巨噬细胞M1到M2表型的极化, M2巨噬细胞比例的升高与肺部炎症有关[37]。PI3K-AKT信号通路也会促进肺部的氧化应激和衰老, 香烟烟雾会刺激肺部细胞大量释放活性氧和活性氮, 在COPD早期诱导内源性氧化应激, 这种氧化应激的升高在慢阻肺患者戒烟后仍然存在, 引起内源性组织和细胞损伤, 从而导致慢性炎症和

衰老[38,39]。Ras蛋白的功能主要在于调节细胞增殖、分化、衰老、细胞凋亡等生命过程, 在细胞信号转导过程中充当着重要的分子开关的作用。有研究表明Ras蛋白是调节上皮间充质转化 (EMT) 的关键节点, 其失活可以抑制EMT过程的发生, 对肺纤维化具有调节作用。Zhang等[40]研究表明, 黄芪甲苷Ⅳ可以通过靶向Ras蛋白下调Ras/FoxO信号通路, 抑制成纤维细胞转化为肌成纤维细胞, 同时减少EMT过程, 来预防与治疗肺纤维化, 从而控制COPD病程的发展并改善呼吸功能。根据关键靶点富集分析结果显示, “用组”主要聚焦在AGE-RAGE通路, 会进一步地引起慢性炎症、氧化应激、血管内皮细胞功能异常, 调控此信号通路可减轻COPD病程中的炎症反应和血管平滑肌细胞异常增殖; 同时可作用于Ras信号通路, 通过减少气道内黏液的分泌和气道重塑, 清除异常的成纤维细胞, 降低COPD肺纤维化的程度, 这与《辅行诀》中所记述的“用”为五脏之功用的理论相对应。“体组”主要聚焦在C型凝集素受体, 与病原体相关分子模式相互作用, 诱导细胞内信号转导, 触发细胞因子的产生, 诱导适应性免疫反应, 以减轻COPD中炎症反应的发生。“化组”主要聚焦在Th17细胞分化、Th1/Th2细胞分化和Toll样受体上, 从不同层面调节炎症通路, 减少肺部中性粒细胞等炎症细胞的浸润, 以减轻气道炎症生成, 改善COPD的临床症状。大补肺汤体–用–化三组合用后作用于MAPK信号通路和EGFR信号通路, 通过调控细胞的存活与增殖、分化、纤维化和黏液分泌来抑制气道成纤维细胞增殖、细胞外基质沉积, 这与气道重塑和纤维化密切相关。研究结果为该方的临床治疗COPD及其体–用–化配伍作用机制研究提供了科学依据和指引。

作者贡献: 宿树兰负责课题总体设计及文章修改等; 刘永琦负责项目总体设计; 段金廒给予研究思路和学术指导; 韩昱负责实验操作、数据处理及论文撰写; 罗月月、黄圣如协助实验完成; 刘培、尚尔鑫负责实验技术指导。

利益冲突: 所有作者均声明不存在利益冲突。

References

[1] Chen D, Long HY, Zhang CX, et al. Interpretation of global strategy for the diagnosis, treatment, management and prevention of chronic obstructive pulmonary disease 2025 report [J]. Chin Gen Pract (中国全科医学), 2025, 28: 1937-1949.

[2] Müller A, Wouters EFM, Burney P, et al. Quality of life associated with breathlessness in the multinational burden of obstructive lung disease (BOLD) study: A cross-sectional analysis [J]. Pulmonology, 2025, 31: 2470566.

[3] Knox-Brown B, Patel J, Potts J, et al. Small airways obstruction and its risk factors in the burden of obstructive lung disease (BOLD) study: A multinational cross-sectional study [J]. Lancet Glob Health, 2023, 11: e69-e82.

[4] Agustí A, Celli BR, Criner GJ, et al. Global initiative for chronic obstructive lung disease 2023 report: GOLD executive summary [J]. Eur Respir J, 2023, 61: 2300239.

[5] Zhai Y, Zhu CM, Zhu TX, et al. Global, regional, and national burden of chronic respiratory diseases, 1990-2021 and predictions to 2035: Analysis of data from the global burden of disease study 2021 [J]. Ann Med, 2025, 57: 2530225.

[6] Chai Y, Ji XM, Huang H. Research on the formula structure of tonic and purging decoctions in Fuxingjue Zangfu Yongyao Fayao [J]. China J Tradit Chin Med Pharm (中华中医药杂志), 2025, 40: 829-831.

[7] Qin CC, Zhang SM, Tian MH, et al. Analysis the theory of five flavors in Fuxingjue Wuzang Yongyao Fayao based on the theory of rhythm space-time view [J]. China J Tradit Chin Med Pharm (中华中医药杂志), 2025, 40: 2106-2110.

[8] Sun H. Exploration and Application of Body and Thought in Auxiliary Verse Medicationto Viscera («辅行诀脏腑用药法要»中体用思想探究及应用) [D]. Lanzhou: Gansu University of Chinese Medicine, 2023.

[9] Li CH, Zhang M, Lin J, et al. Analysis of *in vitro* activity and compatibility of Dunhuang Yifang Dabupi Decoction on gastric cancer based on computer-aided drug design [J]. Acta Pharm Sin (药学学报), 2022, 57: 2087-2100.

[10] Jin R. Theoretical system reconstruction of compatibility principle of traditional Chinese medicine prescriptions from perspective of 'Tang-Ye-Jing-Fa map' [J]. China J Tradit Chin Med Pharm (中华中医药杂志), 2023, 38: 1445-1449.

[11] Luo YY, Han Y, Huang SR, et al. Establishment of UPLC-QTRAP-MS/MS analysis method for 6 active ingredients in Dunhuang Medical Formula Daxiefei Decoction and *in vivo* pharmacokinetics study of normal and COPD model rats [J]. Acta Pharm Sin (药学学报), 2025, 60: 3491-3498.

[12] Fan HS, Liu SJ, Shen WX, et al. Identification of the absorbed components and metabolites of Xiao-Ai-Jie-Du decoction and their distribution in rats using ultra high-performance liquid chromatography/quadrupole time-of-flight mass spectrometry [J]. J Pharm Biomed Anal, 2020, 179: 112984.

[13] Hu YS, Zhang JQ, Xu M, et al. Chemical profiling and comparative analysis of different parts of *Asarum heterotropoides* using SPME-GC-QTOF-MS and LC-Orbitrap-MS [J]. J Pharm Biomed Anal, 2025, 252: 116502.

[14] Ouyang Y, Tang LY, Hu SW, et al. Shengmai san-derived compound prescriptions: A review on chemical constituents, pharmacokinetic studies, quality control, and pharmacological properties [J]. Phytomedicine, 2022, 107: 154433.

[15] Yang K, Qiu J, Huang ZC, et al. A comprehensive review of ethnopharmacology, phytochemistry, pharmacology, and pharma-

cokinetics of *Schisandra chinensis* (Turcz.) Baill. and *Schisandra sphenanthera* Rehd. et Wils [J]. J Ethnopharmacol, 2022, 284: 114759.

[16] Wei ZY, Fang C, Chen K, et al. Rapid screening the chemical components in Jiawei Dingzhi pills using precursor ion selection UHPLC-Q-TOF-MS/MS [J]. Acta Pharm Sin (药学学报), 2024, 59: 2350-2364.

[17] Zhu YF, Tan SZ, Wang HL, et al. Identification of chemical constituents in Yiqi Jianpi Granules by UPLC-Q-TOF-MS/MS [J]. Chin Tradit Herb Drugs (中草药), 2022, 53: 3601-3613.

[18] Yang FY, Xu RL, Niu W, et al. UPLC-Q-TOF-MS analysis of chemical constituents of classical prescription Yiguanjian standard decoction [J]. China J Chin Mater Med (中国中药杂志), 2022, 47: 2134-2147.

[19] He D, Pei XY, Liu B, et al. Lignan contents of *Schisandra chinensis* (Turcz.) Baill. from different origins-a new model for evaluating the content of prominent components of Chinese herbs [J]. Phytomedicine, 2024, 128: 155361.

[20] Lu XM, Zhong LY, Wang S, et al. Effect of processing method on chemical constituents of Rehmanniae Radix: Based on UHPLC-LTQ-Orbitrap MS [J]. China J Chin Mater Med (中国中药杂志), 2023, 48: 399-414.

[21] Xu RL, Fan JT, Dong HM, et al. UPLC-Q-TOF-MS analysis on chemical constituents of classical prescription Huangqi Guizhi Wuwu Tang standard decoction [J]. China J Chin Mater Med (中国中药杂志), 2020, 45: 5614-5630.

[22] An Q, Wu LZ, Liu LL, et al. Identification of chemical constituents in Shengmaiyin (Dangshen Prescription) Oral Liquid by UPLC-Q-TOF-MS/MS [J]. Mod Chin Med (中国现代中药), 2024, 26: 120-136.

[23] Yang XY, Li HY, Lou YQ, et al. *In vitro* and *in vivo* chemical composition analysis of reference sample of Jinshui Liujunjian based on UPLC-Q-TOF-MS/MS [J]. Chin J Exp Tradit Med Formulae (中国实验方剂学杂志), 2026, 32: 166-173.

[24] Lu WS, Wei CJ, Pan XJ, et al. Variations of chemical components in *Inula japonica* by UPLC-MS/MS before and after Honey-frying [J]. China Pharm (中国药房), 2021, 32: 2478-2484.

[25] Zhou H, Lai YY, Zhu YY, et al. Quercetin improves airway remodeling in COPD rats by suppressing phenotypic switch of ASMCs *via* inhibiting the Wnt5a/*β*-catenin pathway [J]. Phytomedicine, 2025, 139: 156491.

[26] Wu ZH, Jia MQ, Zhao WJ, et al. Schisandrol A, the main active ingredient of *Schisandrae Chinensis* Fructus, inhibits pulmonary fibrosis through suppression of the TGF-*β* signaling pathway as revealed by UPLC-Q-TOF/MS, network pharmacology and experimental verification [J]. J Ethnopharmacol, 2022, 289: 115031.

[27] Li JH, Niu LH, Huang H, et al. 1-*O*-Acetylbritannilactone exerts anti-inflammatory and anti-MUC5AC effects by targeting PKC-*α* and downregulating the SRC/EGFR/MAPK signaling pathway [J]. Int Immunopharmacol, 2025, 161: 114979.

[28] Ko HM, Lee SH, Jee W, et al. Gancaonin N from *Glycyrrhiza uralensis* attenuates the inflammatory response by downregulating the NF-*κ*B/MAPK pathway on an acute pneumonia *in vitro* model [J]. Pharmaceutics, 2021, 13: 1028.

[29] Hong JH, Kang MH, Lee JJ, et al. *γδ*(+) T-cell-derived IL-17A stimulates airway epithelial/stromal cells to secrete G-CSF, promoting lung-specific pathogenic Siglec-F(+) neutrophil development in PPE-induced emphysema [J]. Cell Mol Immunol, 2025, 22: 791-805.

[30] Yu JL, Qi JL, Kong XN, et al. Interleukin-11: A central integrative hub driving pathological progression from pulmonary inflammation and fibrosis to cancer [J]. Pharmacol Res, 2025, 221: 107966.

[31] Hsu AT, O'Donoghue RJJ, Tsantikos E, et al. An unconventional T cell nexus drives HCK-mediated chronic obstructive pulmonary disease in mice [J]. EBioMedicine, 2025, 115: 105707.

[32] Cazzola M, Page C, Rogliani P, et al. PI3K inhibitors as potential therapeutic agents for the treatment of COPD with associated atherosclerosis [J]. Drugs, 2025, 85: 741-753.

[33] Zeng XX, Gao DD, Zhang F. Cortex Mori Radicis [*Morus Alba* L. (Moraceae)] extract alleviates senescence *via* PI3K/Akt signaling in COPD fibroblasts [J]. Phytomedicine, 2024, 135: 156004.

[34] Strickson S, Houslay KF, Negri VA, et al. Oxidised IL-33 drives COPD epithelial pathogenesis *via* ST2-independent RAGE/EGFR signalling complex [J]. Eur Respir J, 2023, 62: 2202210.

[35] Wang CX, Zhou JD, Wang JQ, et al. Progress in the mechanism and targeted drug therapy for COPD [J]. Signal Transduct Target Ther, 2020, 5: 248.

[36] Liu YH, Kong HB, Cai HP, et al. Progression of the PI3K/Akt signaling pathway in chronic obstructive pulmonary disease [J]. Front Pharmacol, 2023, 14: 1238782.

[37] Zhang P, Zhang YX, Wang L, et al. Reversal of NADPH oxidase-dependent early oxidative and inflammatory responses in chronic obstructive pulmonary disease by puerarin [J]. Oxid Med Cell Longev, 2022, 2022: 5595781.

[38] Yi XF, Li TT, Wei X, et al. Erythromycin attenuates oxidative stress-induced cellular senescence *via* the PI3K-mTOR signaling pathway in chronic obstructive pulmonary disease [J]. Front Pharmacol, 2022, 13: 1043474.

[39] Xie SL, Wang XF. CRYAB reduces cigarette smoke-induced inflammation, apoptosis, and oxidative stress by retarding PI3K/Akt and NF-*κ*B signaling pathways in human bronchial epithelial cells [J]. Allergol Immunopathol (Madr), 2022, 50: 23-29.

[40] Zhang M, Wang WS, Liu KX, et al. Astragaloside IV protects against lung injury and pulmonary fibrosis in COPD by targeting GTP-GDP domain of RAS and downregulating the RAS/RAF/FoxO signaling pathway [J]. Phytomedicine, 2023, 120: 155066.